

Surface-flow topology of deflected jets through a short cylindrical chamber

S. K. Lee¹ and P. V. Lanspeary²

¹School of Engineering, The University of Newcastle, N.S.W., 2308 AUSTRALIA

²School of Mechanical Engineering, The University of Adelaide, S.A., 5005 AUSTRALIA

Abstract

In the flow under consideration, a jet of fluid emerges from an orifice and then passes through a short cylindrical chamber which has an axis passing through the centroid of the orifice. The cross-section area of the chamber is at least a factor of ten larger than that of the orifice, and the increase in area causes immediate separation at the orifice. A carefully chosen chamber geometry produces an asymmetrically deflected jet. In the first known flow of this kind, the fluidic precessing jet (FPJ), the deflected jet impinges on the cylindrical wall, and the region of impingement precesses around the internal perimeter of the chamber. Visualisation experiments with the oscillating FPJ flow gives only very limited information on the flow topology. However, there are several ways of adjusting the inlet (i.e. orifice) boundary condition and the chamber dimensions so that the deflected jet is stationary. In these non-oscillating flows, the topology of flow at surface of the chamber has been obtained by surface-paste flow visualisation. The flow visualisation shows that topology of the separated flow depends on the chamber-inlet boundary condition. The result is a family of surface-flow topologies. By arranging the topologies into a sequence, we observe that each topology can be converted to the next by removing or adding just one node and one saddle or, in one case, by adding or removing swirl.

Introduction

This article reports an analysis of non-axisymmetric flow through an axisymmetric nozzle. The nozzle consists of a short cylindrical chamber with a concentric inlet at one end and a circular exit lip at the other end. Figure 1 defines the geometric parameters of the nozzle.

This nozzle, with a circular-inlet orifice, length-to-diameter ratio $L/D=2.7$ and abrupt-expansion ratio $D/d_1 \geq 5$ at the inlet [7], produces an oscillating-jet flow. Researchers have long recognised that oscillation can significantly change the mixing characteristics of emerging-jet flow [2, 8], and this is exploited in the design of devices such as ejectors, burners, air-conditioning outlets and rock drills. The nozzle (shown in Figure 1) is used as an industrial natural-gas burner [5].

Investigations by Nathan [7] find that flow from the inlet orifice of the nozzle is deflected asymmetrically and reattaches to the wall of the chamber (Figure 2). The direction of deflec-

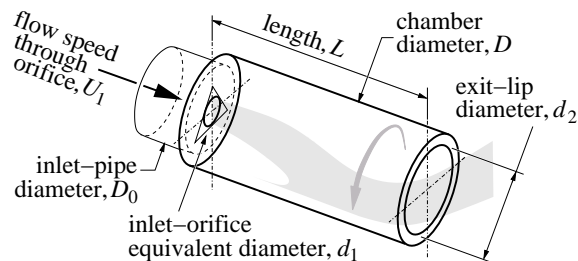


Figure 1: Geometric parameters of the nozzle. Inlet orifices are circular or triangular.

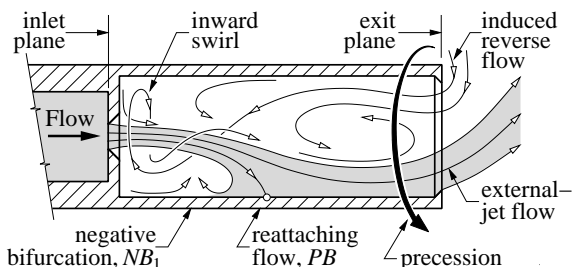


Figure 2: Schematic diagram of flow inside the FPJ nozzle — inferred from flow visualisation.

tion changes with time so that the reattached jet travels or “precesses” around the wall; hence the name “fluidic precessing-jet” or FPJ nozzle. Nathan [7] also observes a reverse flow through the nozzle-exit plane and, in China-clay surface-flow visualisation, identifies a strong swirl adjacent to the inlet plane of the nozzle. The China-clay image in Figure 3 shows the reattachment point as a circumferential positive-bifurcation line, PB . Flow between reattachment and the inlet plane converges to a negative-bifurcation line, NB_1 . These flow features are also shown schematically in Figure 2.

This paper examines internal surface-flow patterns of several variations of the FPJ nozzle. These variations are obtained by changing the inlet-boundary conditions: by tilting the inlet pipe, by changing the shape of inlet from circular to triangular, and by changing the abrupt-expansion inlet orifice into a smooth convergent/divergent inlet.

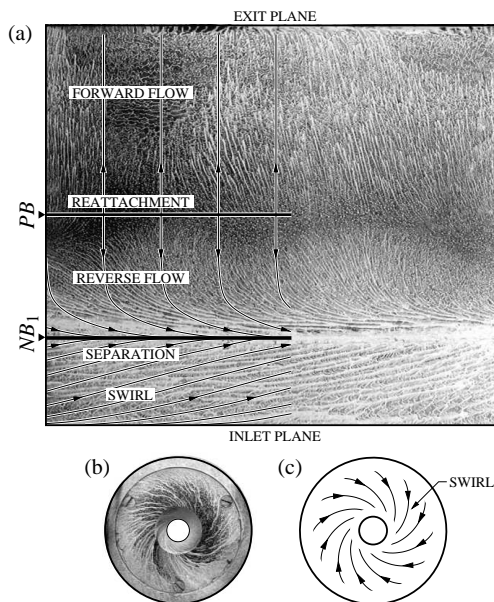


Figure 3: China-clay surface-flow visualisation in the FPJ nozzle and streakline interpretation [7]; (a) on the unwrapped cylindrical surface; (b, c) at the inlet plane. PB and NB_1 are circumferential “rings”. $D/d_1 = 6.4$; $L/D = 2.70$; $Re_1 = 280,000$.

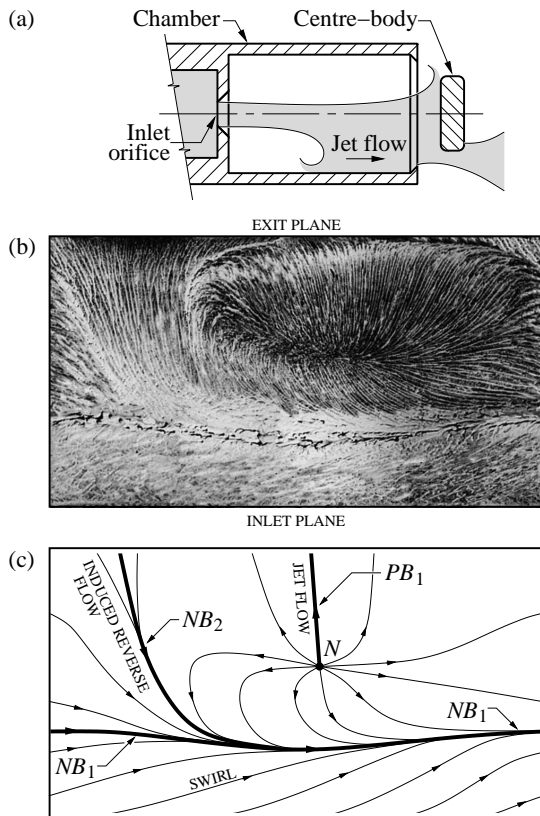


Figure 4: Short cavity FPJ nozzle with an external centre-body; (a) schematic diagram of nozzle; (b) surface-flow visualisation image (unwrapped cylindrical wall) [7]; (c) surface streaklines and interpretation. $D/d_1 = 6.4$; $L/D = 1.68$; $Re_1 = 280,000$.

Short-cavity FPJ nozzle with external centre-body

Nathan [7] obtains surface-flow images from several variations of the standard FPJ geometry. In one case, with a shorter cavity ($L/D = 1.68$) and an external disk or centre-body, the streakline pattern is asymmetric. Nathan [7] suggests that this is due to azimuthal bias in the precession or non-axisymmetry of a long-time-averaged flow. The surface streaklines in the standard FPJ cavity (Figure 3) and in the shorter cavity (Figure 4) both show evidence of swirl adjacent to the inlet plane. However, in the short cavity, the line NB_1 is curved (rather than straight), and the visualisation method shows evidence of a reattachment node N rather than a positive-bifurcation ring PB .

In Figure 4, the path of the jet is indicated by the positive-bifurcation line PB_1 which extends from the reattachment node N to the exit plane. Figure 4 also indicates an induced reverse flow from the exit plane to the line NB_1 . Flow spreading circumferentially away from the node N converges toward the negative-bifurcation line NB_2 which extends from the exit plane to the line NB_1 .

FPJ nozzle with a tilted inlet

Hill [1] prevents precession in the FPJ nozzle by tilting the inlet pipe to an angle of 8° from the axis of the chamber, as in Figure 5(a). Figure 5(b) is a surface-paste visualisation image of the flow. This surface flow is topologically identical to that of Figure 4, but the circumferential line NB_1 is more strongly curved. Perhaps surprisingly, because the deflected jet is stationary rather than precessing, there is swirl between the line NB_1 and the inlet plane. Clearly, swirl is not necessarily a result of precession and swirl is not sufficient to cause precession

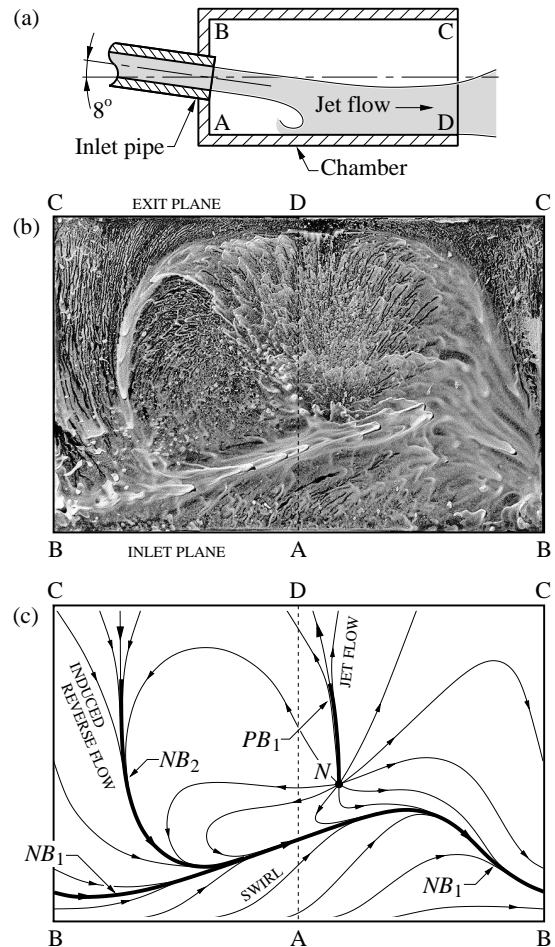


Figure 5: Nozzle with inlet pipe tilted 8° ; (a) schematic diagram of nozzle; (b) surface-flow visualisation image (unwrapped cylindrical wall) [1]; (c) surface streaklines and interpretation. $D/d_1 = 6.0$; $L/D = 2.10$; $Re_1 = 280,000$.

in the FPJ nozzle. The induced reverse flow observed in the short-cavity flow (Figure 4) is also clearly visible in the tilted-inlet-pipe flow (Figure 5), and it includes a negative-bifurcation line NB_2 . A positive-bifurcation line PB_1 lies in the path of the reattached jet.

Hill [1] also found that increasing the angle of tilt from 8° to 20° significantly changes the flow pattern on the surface of the chamber. With 20° of tilt, the flow (Figure 6) is symmetrical about the line \overline{AD} , and there are two negative-bifurcation lines NB_2 and NB_2' , and two foci F_a and F_b . In Figure 6, negative bifurcations NB_2 and NB_2' run from the exit plane to the foci F_a and F_b , respectively. The two foci, one on each side of the jet-reattachment node N , counter rotate and are of the same size. Flow along the circumferential negative-bifurcation line NB_1 no longer runs in just one direction (e.g. from left to right) but reverses direction at saddle points S_a and S_b so that flow between NB_1 and the inlet plane is without swirl. The lack of paste build-up along NB_1 suggests that, compared with the flow shown in Figures 4 and 5, this negative-bifurcation line is quite weak.

Nozzle with smooth convergent-divergent inlet

Vidakovic [9] studies the flow obtained by replacing the abrupt-expansion inlet of the FPJ cavity with a smooth diffuser-like inlet (Figure 7(a)). At inlet-throat Reynolds numbers $Re_1 < 45,000$, the jet flow separates axisymmetrically at the in-

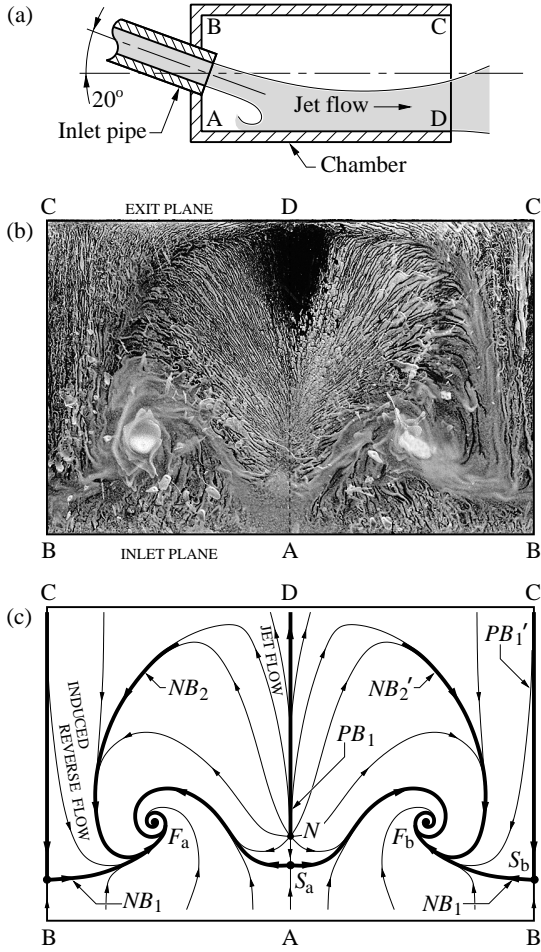


Figure 6: Nozzle with inlet pipe tilted 20° ; (a) schematic diagram of nozzle; (b) surface-flow visualisation image (unwrapped cylindrical wall) [1]; (c) surface streamlines and interpretation. $D/d_1 = 6.0$; $L/D = 2.10$; $Re_1 = 280,000$.

let throat and remains axisymmetric along the length of the chamber. In the range $45,000 \leq Re_1 \leq 55,000$, the flow is intermittently asymmetric and the deflected asymmetric flow remains attached along the length of the chamber. At larger Reynolds numbers the flow “separates asymmetrically and precesses intermittently in an apparently random direction”. Vidakovic suppresses random changes in azimuthal direction by injecting a secondary flow through a small radial port at the throat (i.e. at “B” in Figure 7(a)) of the diffuser. The ratio of secondary-to-primary mass flow rate is no more than 5%. He then studies the stationary-deflected flow through the diffuser using oil-droplet and China-clay flow visualisation.

We now compare surface streamlines in Figure 7 with the symmetrical flow from the 20° -tilted inlet of Hill [1] (Figure 6). Again, there is a stationary deflected jet with two negative-bifurcation lines NB_2 and NB_2' extending back from the exit plane to foci F_a and F_b ; again there is no swirl. However, unlike Figure 6, the jet is continuously attached to the internal surface of the diffuser from the inlet to the exit plane (Figure 7), and so there is no reattachment node (N), there is no adjacent saddle point (S_a) and the negative-bifurcation line (NB_1) is no longer a closed loop — it is an open curve terminating at the foci F_a and F_b . With a convergent-divergent inlet, foci F_a and F_b are the end points of counter-rotating vortices $F_a F_c$ and $F_b F_d$ which are embedded in the turbulent shear layer of the deflected-jet flow.

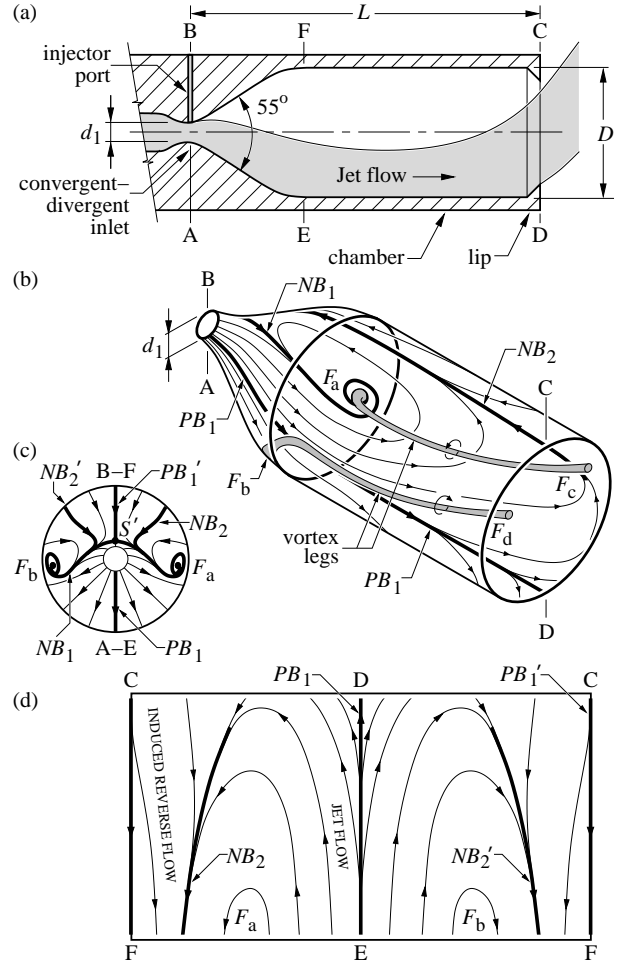


Figure 7: Stationary deflected flow through nozzle with smooth convergent-divergent inlet; (a) schematic diagram of nozzle; (b) surface streaklines and counter-rotating longitudinal vortex legs; (c) internal surface of the diffuser when viewed from nozzle exit [9]; (d) unwrapped cylindrical wall; $D/d_1 = 6.0$; $L/D = 2.70$; $Re_1 = 72,000$.

Stationary-deflected triangular jet

The FPJ nozzle produces an oscillating jet only if the inlet expansion ratio D/d_1 is larger than 5. If the circular inlet of the FPJ is replaced with a triangular inlet, precession or oscillation of the jet is obtained at area expansion ratios as low as 2.0^2 [6]. A parametric study by Lee et al. [4] shows that the spreading angle varies more gradually as a function of L/D ratio than the FPJ spreading angle. The parametric study also shows that, if $D/d_1 = 3.5$ and if the chamber is shortened to $L/D = 1.25$, oscillation ceases and flow emerges from the nozzle as a deflected jet. In this case, d_1 is the diameter of a circle with the same area as triangular orifice.

Lee et al. [3] obtain surface-flow-visualisation images of the “stationary deflected triangular jet” (SDTJ) and report details of its surface-flow topology. Figure 8 shows that this flow has surface features similar to those produced by adding an external centre-body (Figure 4) or by tilting the inlet pipe (Figure 5) — similar swirl, jet reattachment node N , induced reverse flow and bifurcation lines NB_1 , NB_2 and PB_1 . The SDTJ surface flow also has two counter-rotating sink foci F_a and F_b which are of unequal strength. Further experiments [3] show that fluid attracted to the foci is entrained by the jet and is ejected from the chamber as a pair of counter-rotating longitudinal vortices.

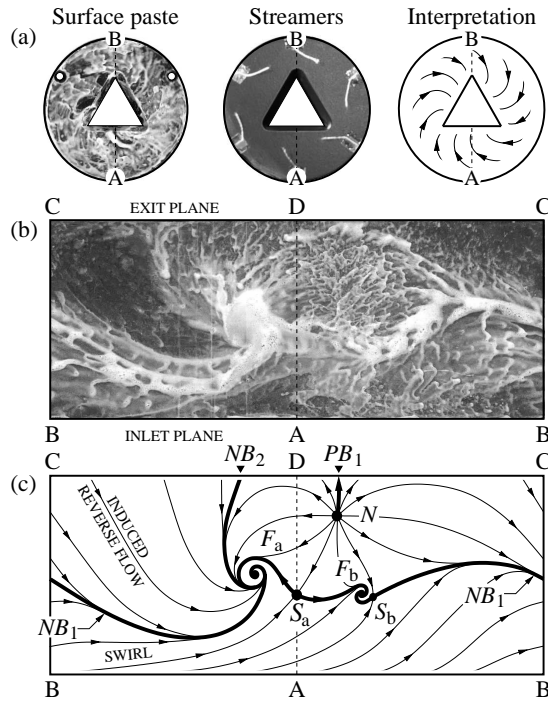


Figure 8: Stationary deflected triangular jet; (a) flow visualisation on the inlet plane; (b) surface-flow visualisation image (un-wrapped cylindrical wall); (c) surface streaklines and interpretation. $D/d_1 = 3.5$; $L/D = 1.25$; $Re_1 = 70,000$.

Discussion

Figure 9 is a summary of the results presented in this paper. The stationary-deflected-triangular-jet (SDTJ) surface flow is shown in Figure 9(c). Figure 9(d) shows a slightly different interpretation of the SDTJ surface-paste image, in which the weak focus F_b and the saddle S_b are removed. As in Figure 9(e), tilting the inlet flow from a circular orifice at an angle of 8° [1] has the effect of removing the focus F_a and the saddle S_a . If the angle of tilt at the inlet is increased to 20° , the flow is most like the SDTJ flow, but it has mirror symmetry about PB_1 and there is no swirl (Figure 9(b)); foci F_a and F_b are of equal strength. If the abrupt expansion at the inlet plane is replaced by a smooth cone [9], “jet” flow from the inlet is deflected but remains asymmetrically attached to the surface along the full length of the chamber, thus removing node N and saddle S_a (Figure 9(a)).

Conclusions

In several non-oscillating deflected-jet flows through a short cylindrical chamber, the topology of the surface flow has been obtained by flow visualisation. The flow visualisation shows that topology of the separated flow depends on the chamber-inlet boundary condition. The result is the family of flow topologies shown in Figure 9. By arranging the topologies into a sequence, we observe that each topology can be converted to the next by removing or adding just one node and one saddle or, in one case, by adding or removing swirl.

References

[1] Hill, S. J., Private communication: surface-flow pattern in a sudden-expansion nozzle, FCT Combustion Ltd., Adelaide, Australia, 2003.
 [2] Knowles, K. and Saddington, A. J., A review of jet mixing enhancement for aircraft propulsion applications, *Journal of Aerospace Engineering*, **220**, 2006, 103–127.

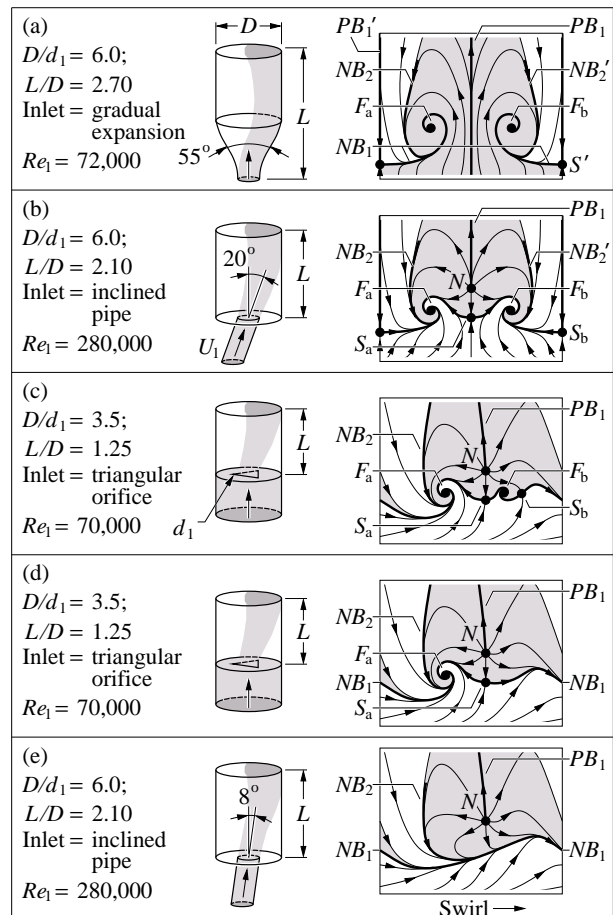


Figure 9: Summary of topologies for stationary deflected jet flows. For each flow, main parameter values are on the left, a sketch of the chamber is shown in the middle, and on the right-hand side is a diagram of surface-flow topology on the un-wrapped inner surface of the chamber.

[3] Lee, S. K., Lanspeary, P. V., Nathan, G. J. and Kelso, R. M., Surface-flow patterns in oscillating-triangular-jet nozzles, in *Proceedings of the 15th Australasian Fluid Mechanics Conference*, paper 52, Sydney, Australia, 2004.
 [4] Lee, S. K., Lanspeary, P. V., Nathan, G. J., Kelso, R. M. and Mi, J., Low kinetic-energy loss oscillating-triangular-jet nozzles, *Experimental Thermal and Fluid Science*, **27**, 2003, 553–561.
 [5] Manias, C. G. and Nathan, G. J., Low NO_x clinker production, *World Cement*, **25**, 1994, 54–56.
 [6] Mi, J., Nathan, G. J., Luxton, R. E. and Luminis Ltd., Naturally oscillating jet devices, Australian Patent Office, Patent Application No. PP0421/97, 1998.
 [7] Nathan, G. J., *The enhanced mixing burner*, Ph.D. Thesis, The University of Adelaide, Department of Mechanical Engineering, Adelaide, Australia, 1988.
 [8] Reynolds, W. C., Parekh, D. E., Juvet, P. J. D. and Lee, M. J. D., Bifurcating and blooming jets, *Annual Review of Fluid Mechanics*, **35**, 2003, 295–315.
 [9] Vidakovic, S. S., *Fluid dynamic means of varying the thrust vector from an axisymmetric nozzle*, Ph.D. Thesis, The University of Adelaide, Department of Mechanical Engineering, Adelaide, Australia, 1995.